# Conducting photopolymers on orthopeadic implants having a switch of priority between promoting osteogenic and antibacterial activity†

***Jingwen Liao, Weiguo Chen, Mingjin Yang, Junli Zhou, Zhengao Wang, Yahong Zhou,Chengyun Ning and Hai Yuan***

## Experimental detail

### Chemicals

All chemicals of analytical grade were purchased from Sigma-Aldrich Co., Ltd., and used without further treatment if not specified otherwise. Chondroitin sulphate (CS) with high and low molecular weight (*ca.* 55,000 and 4,300, respectively) was supplied by Better biotech. CO., Ltd. Synthetic peptide OP-145 with a molecular mass of 3093.82 Da, friendly provided by Yang's group of University of Amsterdam, was preparedby normal 9H-fluorenylmethyloxycarbonyl (Fmoc)-chemistry using preloaded tentagel resin, benzotriazol-1-yl-oxy-tris-pyrrolidino-phosphonium hexafluorophosphate (PyBop)/N-methylmorpholin (NMM) for *in situ* activation and 20% piperidine in NMP for Fmoc removal.

### Photopolymerization of PPy on implants

Ti-5Al-2.5Fe orthopeadic implant sheets (ISO/DIS 5832-10) with 0.5 mm in thickness prior to use were treated ultrasonically in deionized water, ethanol, and acetone, respectively, and polished chemically in a mixed solution with 1:1 (v/v) of 0.8 M HF and 0.3 M $HNO_3$, and followed by multiple rinse using deionized water. A precursor solution containing 0.45 M pyrrole (Py), 0.01 M $AgNO_3$, 0.50 mg/mL CS (low molecular weight) and 0.07 mM OP-145 was spun on implant at 100 rpm for 30 s. Under the exposure of UV-radiation (365 nm) with power density of 5 $mW/cm^2$ for 20 min, PPy incorporated with CS and OP-145 was formed on implants at ambient temperature. The as-obtained PPy/implant specimens were immersed in deionized water with changing per 1 h for at least 5 times to eliminate the unreacted species, and subsequently stored in phosphate buffered saline (PBS) solution prior to use.

### Switch states of PPy/implant controlled by *in situ* electrical stimuli

An electrochemical cell included PPy/implant as working electrode, platinum sheet as counter electrode, saturated calomel electrode (SCE) as reference electrode, PBS

containing 0.2 M NaCl as electrolyte. Under the control of electrochemical station (CH Instrument, CHI 660E, Germany), we herein applied *in situ* electrical stimuli of +0.50 V and -0.50 V for 20 min to trigger oxidation and reduction in the three-electrode system at ambient temperature. The oxidation state was labeled as switch (+0.5 V) while reduction state was termed as switch (-0.5 V). The switch (+0.5 V) and switch (-0.5 V) of PPy/implant were reversibly achieved by applying periodic electrical stimuli.

**Characterization of materials**

Scanning electron microscopy (SEM, Hitachi S-4800, Japan) and atomic force microscopy (AFM, Shimadzu SPM-9600, Japan) were employed to examine surface topography of PPy/implant. Transmission electron microscopy (TEM, JEOL JEM-2100, Japan) was used to observe the size and dispersion of Ag nanospheres incorported in PPy matrix. The crystalline state of PPy/implant was analyzed by X-ray diffraction (XRD, BrukerD8 Advanced, Germany). The surface potentials of PPy/implant in various switch states were characterized using Kelvin probe force microscopy (KFM, Shimadzu SPM-9600, Japan) and electrokinetic analyser (Anton PaarSurPASS, Germany). X-ray photoelectron spectroscopy (XPS, Kratos Axis Ultra DLD, Britain) and energy-dispersive spectroscopy (EDS, Horiba 7593-H, Britain) was utilized to analyze the chemical composition of specimens. The electrochemical activity of PPy/implant was tested by cyclic voltammetry conducted in above-mentioned three-electrode system. Static water contact angle measurements were performed on PPy/implant (dried under vacuum) by surface contact angle analyzer (KSV Helsinki CAM200, Finland) with a 1 μL water droplet at ambient temperature.

**MC3T3-E1 osteoblasts culture and seeding on PPy/implant**

MC3T3-E1 osteoblasts were cultured in α-modified minimum essential medium (α-MEM) supplemented with 10% foetal bovine serum (FBS) in a humid incubator at 37 °C and 5% $CO_2$. Antibiotics (penicillin/streptomycin, P/S) were added to culture media for all cell growth. After the formation of switch states in response to periodic electrical stimuli, the PPy/implant specimens were sterilized by immersion in 70% ethanol for 5 min, followed by drying under a sterile condition and exposing to UV light for 20 min. Specimens were placed into wells of a 48-well polystyrene cell culture plate. MC3T3-E1 osteoblasts were seeded on the specimens at $2 \times 10^3$ cells/cm$^2$, with the medium changed every 2 days. For the proliferation studies, the numbers of adherent cells on the substrates at day 1, day 4 and day 7 were quantified using Cell Counting Kit-8 (CCK-8) assay at 450 nm.

**Observation of MC3T3-E1 osteoblasts on PPy/implant**

To image MC3T3-E1 osteoblasts on specimens by fluorescence staining after they being cultured for predetermined time, cells were fixed in ice-cold 4% paraformaldehyde for 30 min and then washed twice in PBS. Nuclei were stained with DAPI (1 μg/mL) for 10 min at room temperature. F-actin of cells was stained with 50 μg/mL Rhodamine-labeled phalloidin in PBS for 20 min at room temperature. Then the cells were washed three times with PBS to remove unbound phalloidin. Images were acquired under a laser scanning confocal microscope (Zeiss LSM 780, Germany). For morphological observation by SEM, MC3T3-E1 osteoblasts were cultured on specimens, and incubated for 4 h. The specimens were then washed three times with 0.1 M PBS and incubated in 2.5% glutaraldehyde in PBS for 2 h at 4 °C. After washing the specimens using 0.1 M PBS for 3 times, specimens were dehydrated using graded ethanol washes (50, 70, 80, 90, 95 and 100%, 15 min each), and critical-point dried in critical-point dryer (Tousimis Autosamdri-815B, USA). The specimens were gold sputter coated and visualized using SEM.

**Alkaline phosphatase (ALP) activity assay**

Osteogenic media (α-MEM containing 10% FBS, 1% P/S, 10 mM β-glycerophosphate, 0.3 mM L-ascorbic acid and 0.1 μM dexamethasone was added to each well and MC3T3-E1 osteoblasts were incubated for 4, 7 and 14 days. Alkaline phosphatase activity measurement was performed using an alkaline phosphatase assay kit (Abcam). Each replicate was prepared by pooling culture supernatants from three wells. Culture supernatants (30 μL) were combined with alkaline buffer and 50 μL of p-nitrophenyl phosphate and then incubated for 60 min. The reaction was stopped with 20 μL of stop solution (provided in the kit). The absorbance was then measured at 405 nm.

**Real time PCR analysis**

The expressions of osteoblast mRNA gene markers, including osteocalcin (OCN), osteopontin (OPN), bone sialoprotein (BSP) and collagen I (COL1), were determined on specimens cultured with MC3T3-E1 osteoblasts for 7 and 15 days. Total RNA was extracted using an RNeasy mini kit (QIAGEN) as per the manufacturer's instructions. RNA (1 μg) was added to a 20 μL reverse transcription reaction mixture. Real time PCR was performed according to the method described by the manufacturer: 45 cycles of 95 °C for 30 s, 60 °C for 30 s, and 72 °C for 30 s. Glyceraldehyde-3-phosphate dehydrogenase was used as the housekeeping gene. Quantification of gene expression was based on the CT value for each specimen, calculated as the average of three replicate measurements, and each replicate was

prepared by pooling cell lysates from three wells.

**Bacterial Maintenance and Culture**

Gram-positive *Staphylococcus aureus* (*S. aureus*, ATCC 25923) and Gram-negative *Escherichia coli* (*E. coli*, ATCC 25922) were chosen as bacteria models to assess the antibacterial ability of specimen. Both of them were cultured in lysogeny broth (LB) medium (1% w/v tryptone, 0.3% w/v yeast extract, and 0.5% w/v NaCl). The bacterial pellet obtained from ATCC was rehydrated in 0.5 mL of LB, and several drops of the suspension were immediately placed and streaked on an agar slant of LB. The agar-plate was then incubated aerobically at 37 °C for 24 h. Overnight cultures of *S. aureus* and *E. coli* were made by aseptically transferring a single colony forming unit (CFU) into 10 mL of LB, followed by aerobic incubation under shaking at 200 rpm (37 °C) for 16 h.

**Observation of bacterial adhesion on PPy/implant**

Bacteria from the overnight cultures were used to inoculate fresh media to a final concentration of $10^5$ CFU/mL. Bacteria were then incubated in the same manner as the overnight cultures, until they reached the mid log phase as determined by optical density measurement at 600 nm. Then, the cultures were centrifuged at 4000 rpm for 5 min (Sorvall RC 5B Plus Centrifuge) and followed by removing the supernatant. The bacterial pellet was resuspended in 500 μL of LB. This suspension was then transferred to a 2 mL centrifuge tube and centrifuged at 5500 rpm for 3 min (Fischer Scientific AccuSpin Micro Centrifuge). The supernatant was carefully removed, and the bacterial pellet was resuspended in sterile PBS to a final concentration of $10^6$ CFU/mL. Then, 1 mL of suspension was added to each well containing a specimen and incubated under shaking at 200 rpm (37 °C). After 2 h incubation, first the bacterial suspension was removed, and then the surfaces were washed two times with 1 mL of PBS by pipetting. At the end of the experiment, adherent bacteria on specimens were fixed with 500 μL of 2% glutaldehyde for 30 min, followed by dehydration in a series of increasing alcohol baths (50% ethanol for 10 min, 70% ethanol for 10 min, 90% ethanol for 10 min, followed by a 1 mL wash with 100% ethanol). For visualization of bacterial adhesion on specimen, 500 μL of 5 μM SYTO9 Green Fluorescent Nucleic acid stain (Invitrogen, S3485) was added to each well containing a specimen, protected from light, and incubated for 20 min. Specimens were then washed 3 times with 1 mL of PBS by pipetting the PBS up-and-down twice. Following, the specimens were secured onto a clean microscope slide and viewed under a Fluorescent Microscope (Nikon Eclipse TE2000-U, Japan).

**Antibacterial rate of PPy/implant**

The specimens were incubated in 1 mL of bacterial suspension with a concentration of $10^6$ CFU/mL at 37 °C for 24 h. PBS was used to gently rinse thrice each specimen in order to eliminate non-adherent bacteria, and adherent ones were ultrasonically (40 W) detached in 1 ml of PBS for 5 min. The bacteria suspensions were re-incubated on LB agar plates at 37 °C for 24 h, and the viable bacteria was quantified through colony counting. The antibacterial rates were determined by the following relationship: Antibacterial rate (%) = (CFU of control − CFU of specimens)/CFU of control × 100%, where blank polystyrene plate served as control.

**Statistical analysis**

The surface coverage and spreading area per cell on corresponding fluorescence images were quantified by Image J software (National Institutes of Health 1.49q, USA) Statistically significant differences between groups for osteogenic activity test were assessed using single-factor analysis of variance (ANOVA) with post hoc multiple comparisons tests ($p< 0.05$) (IBM SPSS Statistics, USA). Tukey–Kramer or Dunnett's T3 post hoc tests were used, for equal variances assumed or not-assumed, respectively.

## The other supplementary Information

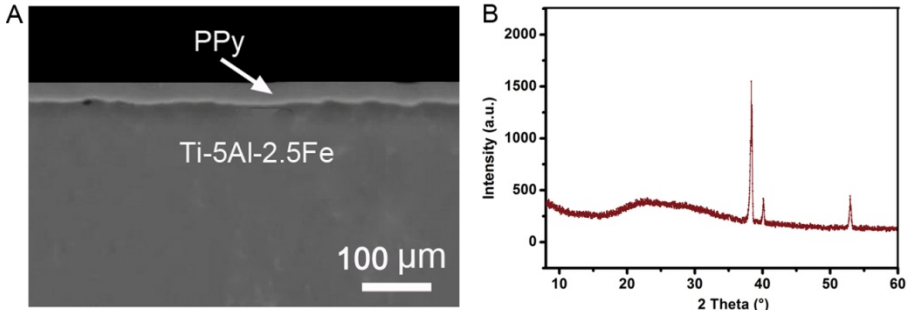


Fig. S1 (A) SEM image of cross section and (B) XRD spectrum of PPy/implant. A PPy film with about 45 μm in thickness was tightly coated on implants. After undergoing 10 tape tests (according to the standard ASTM D 3359-2009), PPy films were not found peeled off from implants, thus showing a good adhesion on implants. In addition, PPy film on implant showed a very broad peak at approximately 24° of 2 theta angle, suggesting its amorphous nature (the three characteristic peaks at 38.4°, 40.1° and 53.0° of 2 theta angles were assigned to Ti-5Al-2.5Fe implant).

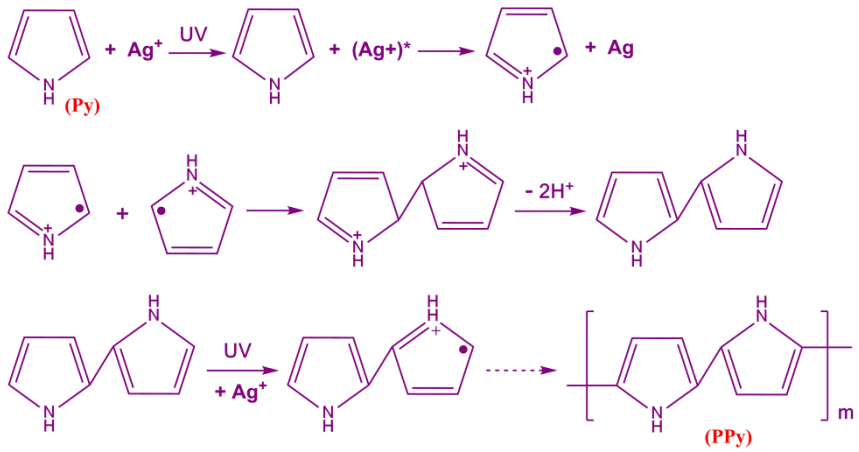


Fig. S2 The mechanism process of UV-induced polymerization of Py in the presence of an $AgNO_3$ photoinitiator. The first stage of cationic polymerization is the excitation of $Ag^+$ upon UV-irradiation (365 nm), making it an easy transfer of an electron (oxidation) from the Py monomer to $Ag^+$ (excitation state). This eventually results in the formation of a Py cationic radical and Ag reduzate in metallic state. The Py radicals then undergo a polymerization process involving dimerization (second stage) and chain growth (third stage).

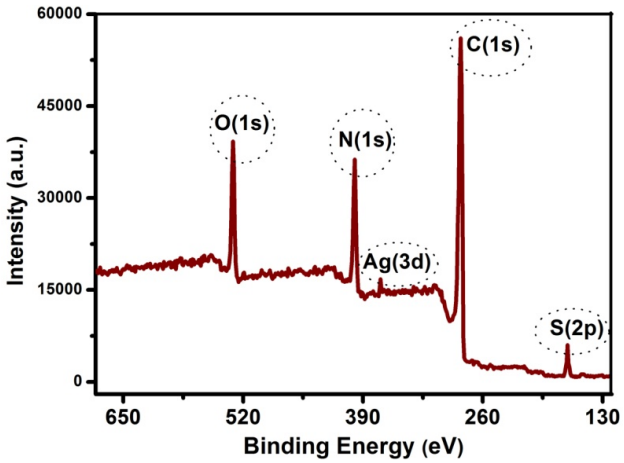


Fig. S3 XPS spectrum of PPy films. Prior to XPS analysis, PPy films were peeled off from implants in a damaged way. Three strong peaks of *O* (oxygen), *N* (nitrogen) and C (carbon) might generally be attributed to the chemical composition of PPy, CS and OP-145. A weak peak of Ag corresponded to Ag reduzate formed during photopolymerization (saw Fig. S2). As to the peak of *S* (sulphur), it could only be assigned to the $SO_3^-$ of CS, indicating the incorporation of CS in photopolymerized PPy matrix. In the "Experimental detail" section, we could find the formation of PPy films on the surfaces of implants under 0.45 M of Py, 0.50 mg/mL of CS, 0.07 mM of OP-145, thus the total strength of *N* peak was mainly related with the amount of *N* element in PPy and CS. Because the ratio of *S* and *N* in CS unit is 1:1, $N_{Py}$ ($N_{Py}$ value:

the number of *N* element of Py) can be calculated by the formula: $N_{total}$- $S_{CS}$ ($N_{total}$: the total number of *N* element of Py and CS, $S_{CS}$ value: the number of *S* element of CS). Given this fact, $S_{CS}/N_{Py}$ could accurately represent the surface density of CS in the PPy matrix. It was found that $S_{CS}/N_{Py}$ of PPy film surfaces was 0.0015, *i.e.*, 15 disaccharide units (CS chains are composed of repeats of disaccharide units) were incorporated in 10,000 Py units (in the form of PPy chain). Because no exclusive chemical element of OP-145 can be used to differentiate from PPy and CS, it is difficult for OP-145 to be quantifiable in PPy films.

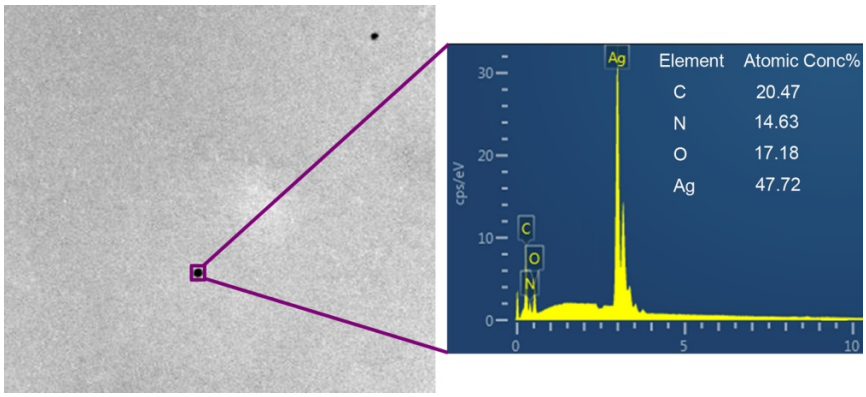


Fig. S4 EDS pattern recorded form selected region of TEM image of photopolymerized PPy. The main element of selected region was Ag, revealing that nanospheres dispersed in PPy matrix was Ag reduzate. It was noteworthy that, the other three elements of *C*, *N* and *O* were visibly detected while S element was not found, due to the amount of CS in the selected region lower than limit of detection of EDS technique.

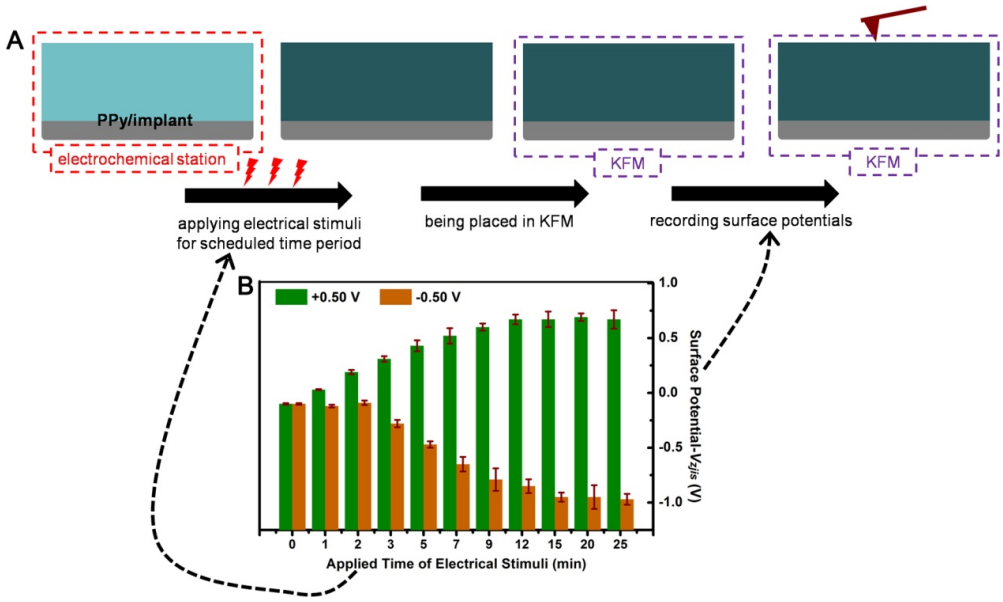

Fig. S5 (A) Schematic illustration of recording process of surface potential of PPy/implant after response to electrical stimuli. (B) The plot of surface potential of PPy/implant *versus* applied time of electrical stimuli. After response to a scheduled time period of the electrical stimuli which were applied to the PPy/implant, the PPy/implant was placed in KFM for recording its surface potentials (no electrical stimuli were applied in recording the surface potentials including the below-mentioned ones). When applying an electrical stimulus of +0.50 V to the PPy/implant in original state, the surface potentials of the films gradually positively increased with the applied times and became stable at 12 min. Conversely, the surface potentials of films gradually negatively increased with the applied times of -0.50 V and remained almost unchanged at 15 min. Therefore, an applying time period of 20 min of electrical stimuli was appropriate for achieving stabilization of surface potentials in oxidation state or reduction state of the PPy/implant.

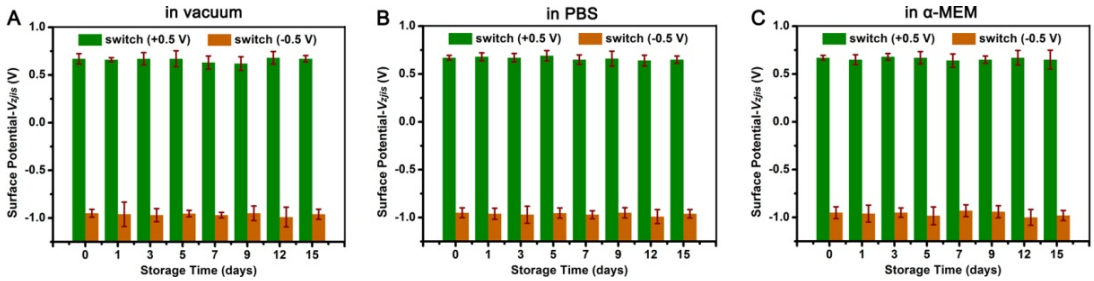


Fig. S6 The plots of surface potential of PPy/implant *versus* storage time (after the electrical stimuli were no longer applied) in (A) vacuum, (B) PBS and (C) α-MEM. Except for storage in vacuum, after the storage in PBS and α-MEM, the specimens were rinsed ultrasonically with deionized water and subsequently dried at room temperature prior to characterization in KFM. Irrespective of the storage conditions, the surface potentials of PPy/implant in both switch (+0.5 V) and switch (-0.5 V) stayed almost unchanged during the 15 days of the storage times. That was, once the formation of switch states through 20 min of applied electrical stimuli, the surface potentials of both switch (+0.5 V) and switch (-0.5 V) enjoyed a long-term stability. In addition, the film adhesion of PPy/implant stored in vacuum, PBS and α-MEM for 15 days was measured by tape test (according to the standard ASTM D 3359-2009). As expected, through undergoing 10 tape tests, PPy films were not found peeled off from implants, thus showing a good adhesion on implants after long-term storage in different conditions.

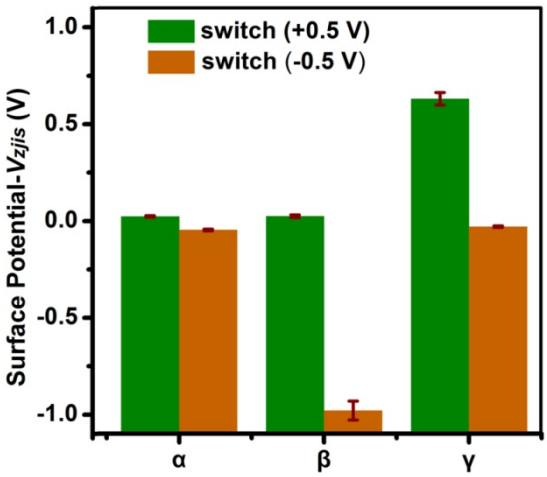


Fig. S7 The plot of surface potential of PPy/implant with various incorporations. α: PPy/implant without incorporation of both CS and OP-145; β: PPy/implant with exclusive incorporation of CS; γ: PPy/implant with exclusive incorporation of OP-145. The surface potentials of PPy/implant with no incorporation of both CS and OP-145 approached 0 V in both switch (+0.5 V) and switch (-0.5 V), and approximately 0 V of surface potentials were also read in PPy/implant with exclusive incorporation of either CS in switch (+0.5 V) or OP-145 in switch (-0.5 V). But much positively or negatively higher surface potentials (+0.63 V and -0.98 V, close to +0.67 V and -0.96 V shown in Fig. 2B) were recognized in PPy/implant with exclusive incorporation of either CS in switch (-0.5 V) or OP-145 in switch (+0.5 V). Therefore, we could conclude that surface positive and negative potentials of PPy/implant were independently derived from positively charged OP-145 and negatively charged CS, respectively.

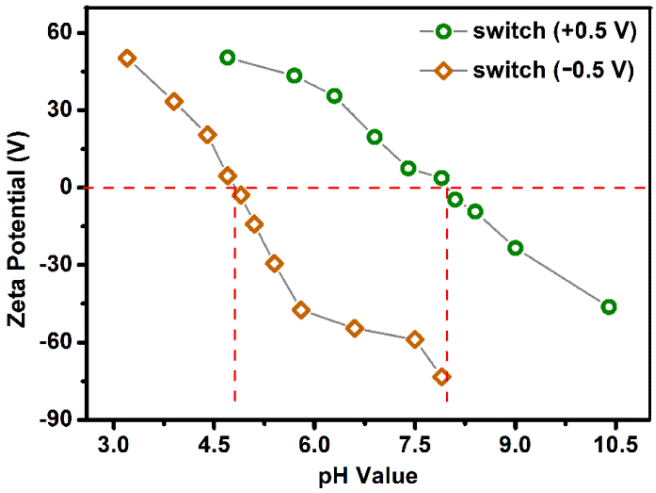


Fig. S8 The plots of zeta potential of PPy/implant in switch (+0.5 V) and switch (-0.5 V) *versus* pH value. The solid surface isoelectric points of PPy/implant were at pH

value of 8.0 in switch (+0.5 V) and 4.8 in switch (-0.5 V). That was to say, the surfaces of PPy/implant were positively charged in switch (+0.5 V) and negatively charged in switch (-0.5 V) in PBS with pH value of 7.4, which is possibly related to the preferential presence of between OP-145 and CS after applying potentials of +0.50 V and -0.50 V, respectively.

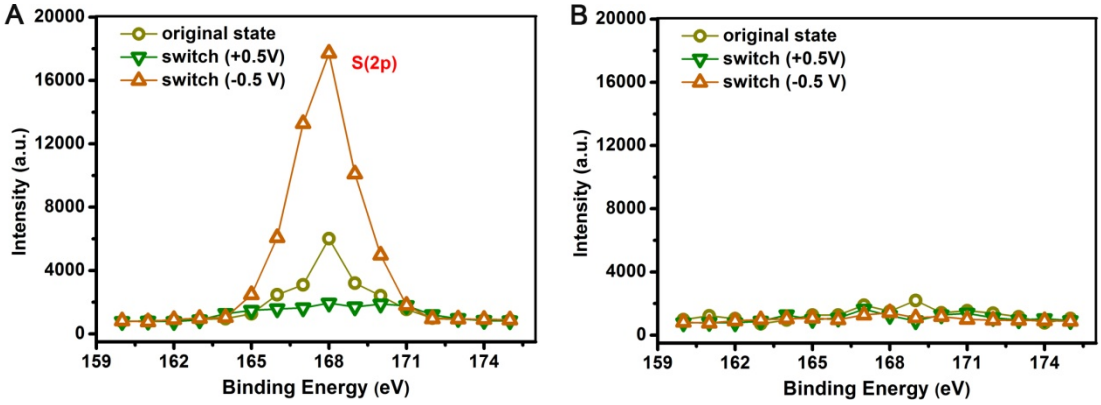


Fig. S9 XPS S (2p) core-level spectra of PPy/implant (A) with and (B) without incorporation of both CS and OP-145 in various switch states. The working depth of XPS technique is generally less than 10 nm, thus can uncover the chemistry of the outmost layer of specimens. In PPy/implant with incorporation of both CS and OP-145, it was disclosed that, the peak strength of *S* was the greatest in switch (-0.5 V) while being negligible in switch (+0.5 V). When no CS and OP-145 was incorporated, *S* peaks were not found in all the three switch states of PPy/implant. Therefore, we could concluded that (a) *S* peak was originated from CS, (b) CS was forced to transport to PPy film surfaces by applying a potential of -0.50 V, and was gradually moved away from the surfaces (*i.e.*, migrated to implants) by applying a potential of +0.50 V. Logically speaking, because of the electric charge of OP-145 having the opposite of CS, the transportation of OP-145 within the PPy matrix was simultaneously conducted in the opposite direction of CS movement, verified by Fig. 2B, 2C and 2D.

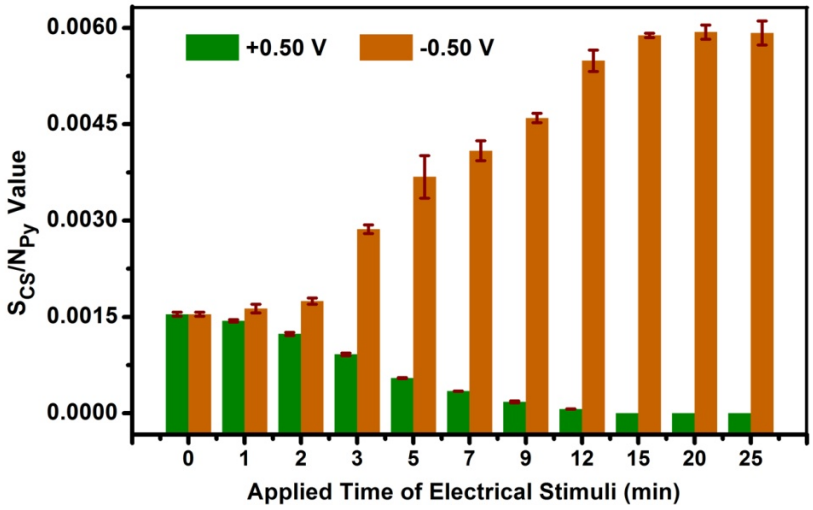


Fig. S10 The plot of $S_{CS}/N_{Py}$ value of PPy/implant surfaces *versus* applied time of electrical stimuli. After response to a scheduled time period of the electrical stimuli which were applied to the PPy/implant, the PPy/implant was placed in XPS for recording its surface chemistry (no electrical stimuli were applied in the recording). When applying an electrical stimulus of +0.50 V to the PPy/implant in original state, the $S_{CS}/N_{Py}$ values of film surfaces gradually decreased until approaching 0 when the applied times were more than 15 min. Conversely, the $S_{CS}/N_{Py}$ values gradually increased with the applied times of -0.50 V and remained almost unchanged at 15 min. It could be seemed that the change rule of $S_{CS}/N_{Py}$ values (*i.e.*, CS density on the PPy/implant surface) was similar to that of surface potentials shown in Fig. S5B. In fact, the change of $S_{CS}/N_{Py}$ values or surface potentials was a reflection of surface rearrangements of CS and OP-145 by their transportation in response to electrical stimuli. Specifically, when applying an electrical stimulus of +0.50 V, one surface rearrangement occurred, that was, CS was forced to gradually migrate to the implants and resulted in less and less CS on the PPy film surfaces, and meanwhile OP-145 was expelled to the PPy film surfaces. In another surface rearrangement when applying an electrical stimulus of -0.50 V, CS was forced to gradually move to the PPy film surfaces where, thus, more and more CS appeared, and meanwhile OP-145 was expelled to in the direction of implants.

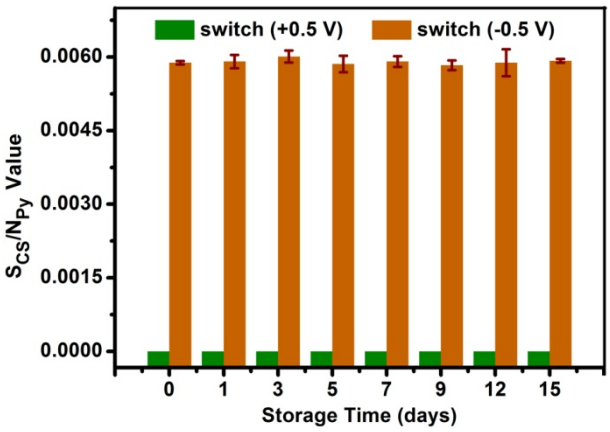


Fig. S11 The plot of $S_{CS}/N_{Py}$ value of PPy/implant surfaces *versus* storage time in vacuum after the electrical stimuli were no longer applied. The $S_{CS}/N_{Py}$ values of the surfaces of PPy/implant in both switch (+0.5 V) and switch (-0.5 V) stayed almost unchanged during the 15 days of the storage times. That was, the surface rearrangements of CS and OP-145 on the PPy films had a good durability after the electrical stimuli were no longer applied.

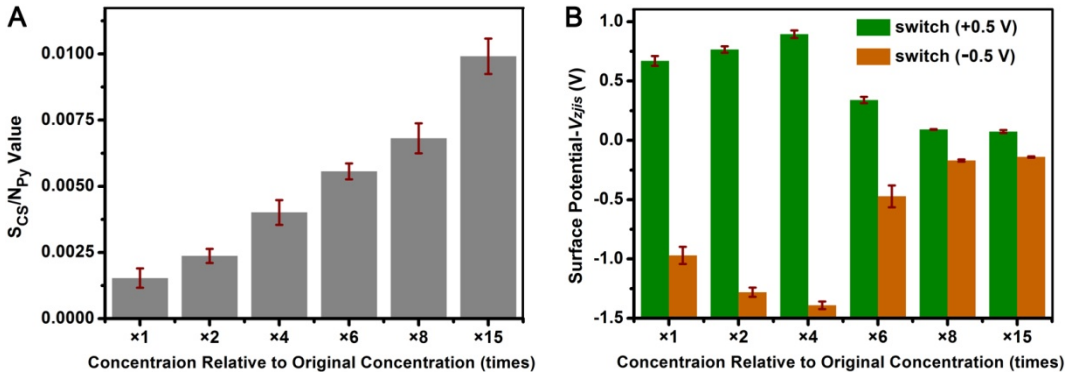


Fig. S12 The plots of (A) $S_{CS}/N_{Py}$ value of PPy/implant surfaces and (B) surface potential of PPy/implant *versus* concentration of CS and OP-145 used in fabrication of PPy on implants. By changing the concentration of CS and OP-145 in photopolymerization of Py, a series of PPy/implant with various incorporation amounts of CS and OP-145 were obtained. As expected, the $S_{CS}/N_{Py}$ value of PPy/implant surfaces was raised from 0.0015 to 0.0059 with the concentration from 1 to 15 times of original concentration of CS and OP-145, indicating that more CS (and more OP-145) were incorporated and thus randomly emerged on the surfaces of PPy/implant. Because more CS and OP-145 could be guided to the PPy/implant surfaces by applying electrical stimuli, the surface potentials of the PPy/implant in switch (+0.5 V) and switch (-0.5 V) were increased in a positive and negative direction, respectively. However, when the PPy/implant was formed by a concentration ranging from 4 to 15 times of original concentration, the surface

potentials of the PPy/implant in switch (+0.5 V) and switch (-0.5 V) were substantially decreased in a positive and negative direction, respectively, and thus gradually approached 0 V. The networks of the PPy polymeric chains showed a stereo-hindrance effect, therefore, CS and OP-145 were separated individually by a certain distance. The distances between CS and OP-145 could be regulated by their incorporation amounts in PPy matrix. When the incorporation amount of CS and OP-145 in the PPy matrix exceeded a specific level, the distance between CS and OP-145 became lower than a critical value. The electrostatic interaction was strong enough to make CS and OP-145 bypass the stereo-hindrance and consequently bind them together. The binding of negatively charged CS and positively charged OP-145 in the PPy matrix brought about an electroneutrality, which resulted in a failure of surface rearrangement of CS and OP-145 on the PPy/implant in response to electrical stimuli. Herein, the surface density of CS (*i.e.*, $S_{CS}/N_{Py}$ value) on the PPy/implant was used to indirectly represent the distance between CS and OP-145 in the PPy matrix. It could be estimated that CS and OP-145 could be separated individually in the PPy matrix by stereo-hindrance of PPy polymeric chains only if the distance between CS and OP-145 was not higher than 0.0040 of $S_{CS}/N_{Py}$ value of the PPy/implant surfaces in original state. That was to say, the surface rearrangements or the preferential presence of either CS or OP-145 on the PPy/implant surfaces could not be achieved in response to electrical stimuli when the freshly prepared PPy/implant was with a $S_{CS}/N_{Py}$ value higher than 0.0040.

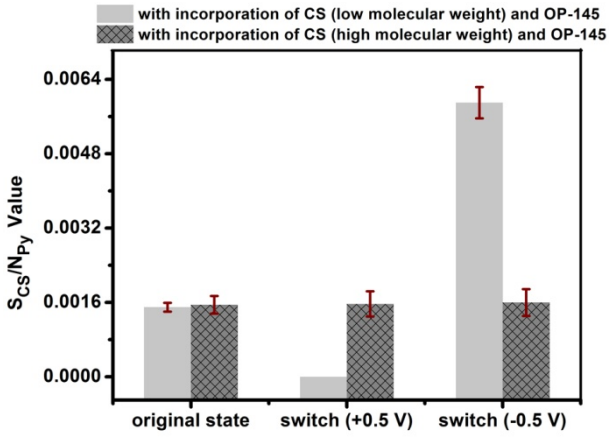


Fig. S13 The plot of $S_{CS}/N_{Py}$ value of PPy/implant surfaces *versus* switch state of PPy/implant. The aforementioned CS incorporated in PPy/implant was with low molecular weight (*ca.* 4,300). Herein, a high molecular weight (*ca.* 55,000) of CS was introduced in PPy matrix in conjunction with OP-145, with an aim to ascertain the effect of molecular weight of incorporation molecules on the resistance against

stereo-hindrance in the migration of incorporation molecules within PPy matrix. Compared with the expected change in the $S_{CS}/N_{Py}$ values of the surfaces of PPy/implant with incorporation of CS (low molecular weight) and OP-145 in various switch states, it was found that, on the surfaces of PPy/implant with incorporation of CS (high molecular weight) and OP-145, the $S_{CS}/N_{Py}$ value in both switch (+0.5 V) and switch (-0.5 V) stayed the same as that in original state, which was due to too high resistance against stereo-hindrance for CS with high molecular weight to migrate within the PPy matrix in response to electrical stimuli and thus seemed entangled in the PPy polymeric chains.

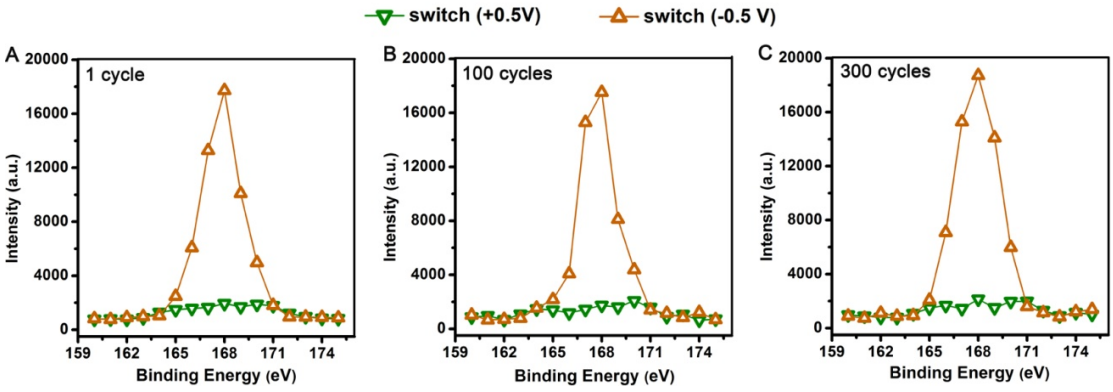


Fig. S14 XPS S (2p) core-level spectra of PPy/implant in switch (+0.5 V) and switch (-0.5 V) after (A) 1, (B) 100 and (C) 300 cycles of applying periodic electrical stimuli to PPy/implant. Through 300 cycles of periodic electrical stimuli, the strength of S peak in XPS spectra of PPy/implant in both switch (+0.5 V) and switch (-0.5 V) stayed almost unchanged, suggesting no release of CS from PPy matrix during continuous switching.

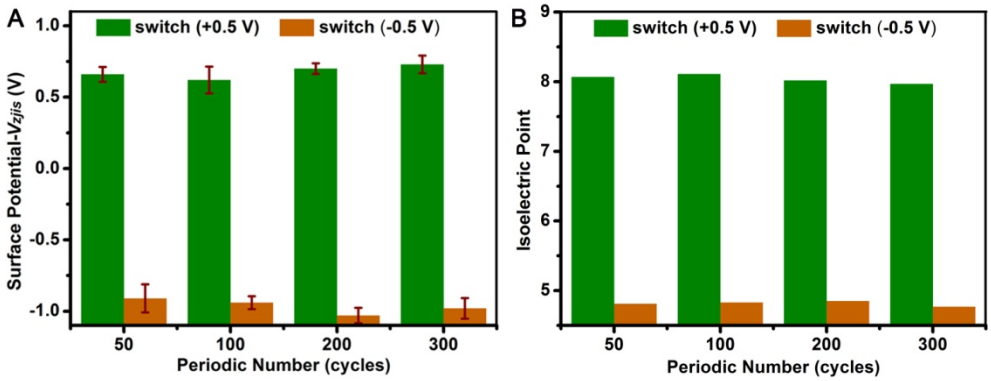


Fig. S15 The plots of (A) surface potential and (B) isoelectric point of PPy/implant in switch (+0.5 V) and switch (-0.5 V) *versus* cycle number of applying periodic electrical stimuli to PPy/implant. It was shown that both surface potentials and

isoelectric points of PPy/implant in both switch (+0.5 V) and switch (-0.5 V) remained relatively stable during the 300 cycles of periodic electrical stimuli, indicating a good stability of electrical stimulus-induced switch of PPy/implant. The good stability of switch activity also provided direct evidence that no CS was released from PPy matrix during continuous switching. In another words, the lifetime of switch behaviours of PPy/implant was long enough and consequently qualified for long-term response of implants.

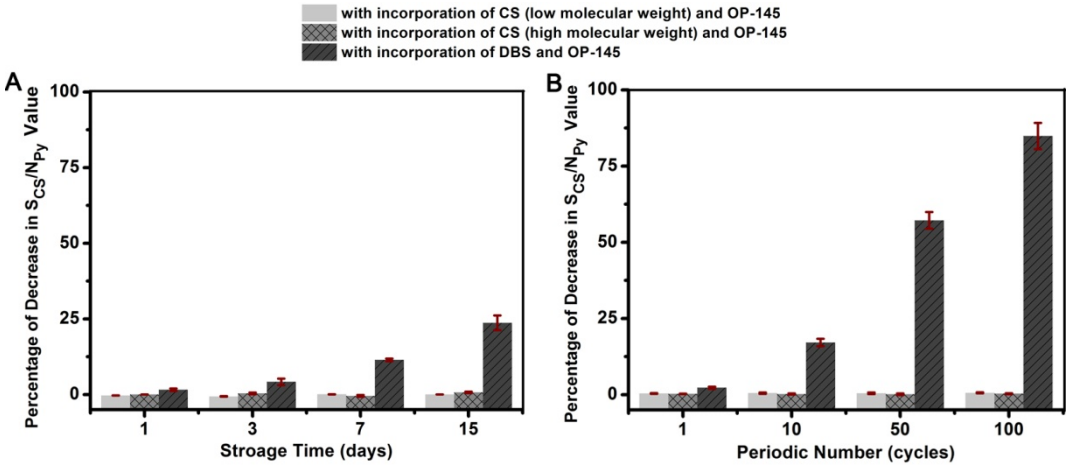


Fig. S16 The plots of percentage of decrease in $S_{CS}/N_{Py}$ value of PPy/implant surfaces *versus* (A) storage time of PPy/implant in PBS and (B) cycle number of applying periodic electrical stimuli to PPy/implant. As a smaller molecule model of CS, the dodecyl benzene-sulfonate (DBS) with molecular weight of *ca.* 300 was incorporated in PPy/implant in conjunction with OP-145. The PPy/implant with incorporation of DBS and OP-145 was immersed in PBS for 15 days. Different from the PPy/implant with incorporation of CS (low or high molecular weight) and OP-145, DBS was found released from the PPy matrix by degrees when the PPy/implant with incorporation of DBS and OP-145 was immersed in an aqueous solution. Similarly, the amount of DBS on PPy/implant surface declined step by step during the responses to periodic electrical stimuli. This was because of too low resistance against stereo-hindrance for small molecule DBS to migrate within the PPy matrix in response to electrical stimuli, and thus DBS was prone to diffusing actively and being ejected passively to aqueous solution.

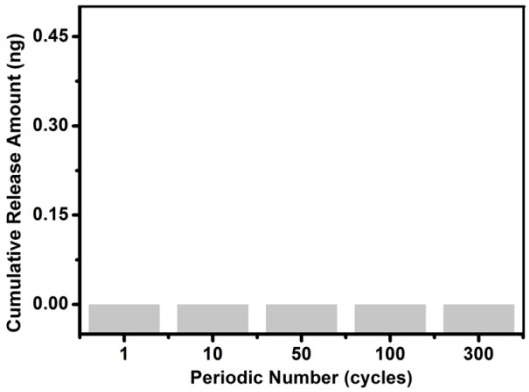


Fig. S17 The plot of cumulative release amount of OP-145 *versus* cycle number of applying periodic electrical stimuli to PPy/implant. The release behaviours of OP-145 from the PPy/implant in PBS in response to periodic electrical stimuli were measured using ultraviolet-visible (UV/Vis) spectroscopy by recording the absorption peak at 257 nm (the characteristic excitation wavelength of phenylalanine). After the response to a specific cycle number of applying periodic electrical stimuli to PPy/implant, the concentrations of OP-145 in PBS were analyzed using a UV/Vis spectroscopy to assess the cumulative release amount. Even though 300 cycles of periodic electrical stimuli were applied, no release of OP-145 from the PPy/implant could be detected. The OP-145 has not much difference of the molecular weights from CS (low molecular weight), which accounts for the same migratory behaviours as CS (even though the transportation of OP-145 is simultaneously conducted in the opposite direction of the CS movement), that is, OP-145 can overcome the stereo-hindrance and migrate within the PPy matrix but not through its surfaces in response to electrical stimuli.

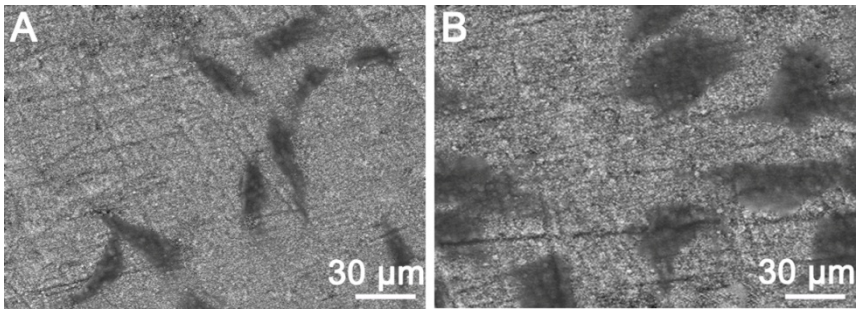


Fig. S18 SEM images of MC3T3-E1 osteoblasts (cultivation of 1 day) on PPy/implant in (A) switch (+0.5 V) and (B) switch (-0.5 V). The osteoblasts were seeded on PPy/implant in switch (+0.5 V) for 1 day, and kept theirs morphologies in rectangle (or spindle) and triangle (or rhombus) and exhibit relatively small spreading area. By contrast, osteoblasts on PPy/implant in switch (-0.5 V) had a larger spreading area and

better spreading morphology.

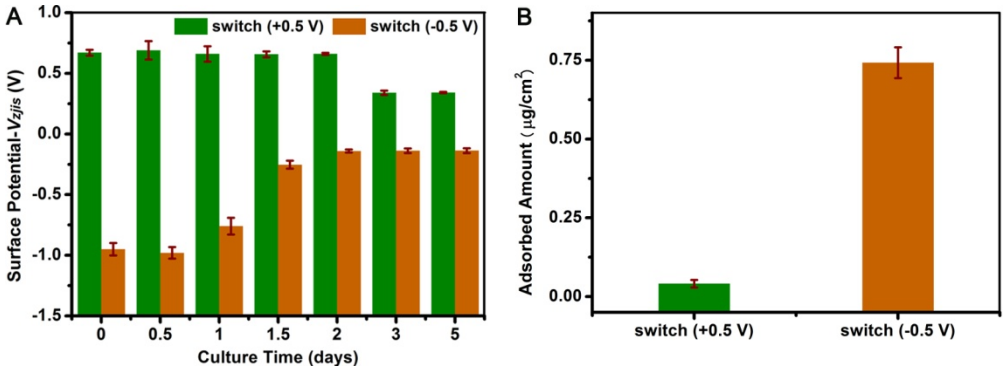


Fig. S19 (A) The plot of surface potential of PPy/implant in switch (+0.5 V) and switch (-0.5 V) *versus* culture time of MC3T3-E1 osteoblasts on PPy/implant. (B) The plot of adsorbed amount of fibronectin on PPy/implant in switch (+0.5 V) and switch (-0.5 V). The PPy/implant in switch (+0.5 V) and switch (-0.5 V) was immersed in α-MEM containing osteoblasts. And subsequently, the specimens were rinsed ultrasonically with deionized water and dried at room temperature prior to the characterization in KFM. With culture times of osteoblasts on the PPy/implant, the surface potentials of switch (-0.5 V) began to negatively decline at 1-day, while the surface potentials of switch (+0.5 V) started to positively lower after 3-day. The PPy/implant in switch (+0.5 V) and switch (-0.5 V) was incubated in fibronectin solution (with 10 μg/mL of fibronectin) at 37 ℃ for 36 h. Then the fibronectin solution was removed, followed by shaking the specimens in 1 wt% sodium dodecylsulfate (SDS) to elute the adsorbed fibronectin. The amount of the adsorbed fibronectin on the PPy/implant surfaces was determined by bicinchoninic acid (BCA) assay. The absorbance of the eluent was measured at 562 nm by a microplate reader (Thermo Scientific Varioskan Flash, USA) with at least three repetitions for each group. It was found that the adsorbed amount of fibronectin on PPy/implant in switch (-0.5 V) was much higher than that in switch (+0.5 V). CS as a naturally osteocytes-philic biomacromolecule was preferentially exposed on the surface of PPy/implants in switch (-0.5 V), which make the surface more attractive to protein adsorption. So it seemed that the surface potentials of switch (-0.5 V) getting changed earlier was derived from more primary stage proteins (such as fibronectin) adsorbing on its surfaces. In fact, before the beginning of the change in surface potentials, there should still be a certain amount of proteins on the PPy/implant surfaces in switch (+0.5 V) or switch (-0.5 V). Such these proteins were prone to being removed from specimens by rinsing ultrasonically with deionized water prior to characterization in KFM, thus no changes in surface potentials of PPy/implant (immersing in α-MEM

containing osteoblasts) could be found in previous 0.5 day for switch (-0.5 V) and 2 days for switch (+0.5 V).

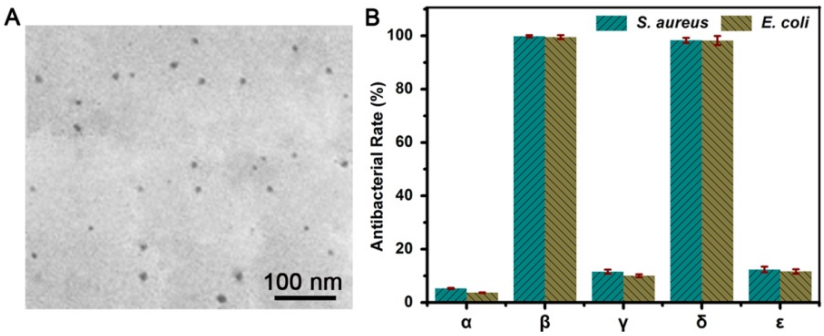


Fig. S20 (A) TEM image of photopolymerized PPy formed under the presence of 0.1 M $AgNO_3$ (as 10 times to the concentration in preliminary scheme). (B) The plot antibacterial rate of bare implant (α), PPy/implant in switch (+0.5 V) (β), PPy/implant in switch (+0.5 V) without incorporating OP-145 (γ), PPy/implant in switch (+0.5 V) with 10 times of original amount of Ag nanospheres (δ), PPy/implant in switch (+0.5 V) with 10 times of original amount of Ag nanospheres and without incorporating OP-145 (ε). We designed several groups of PPy/implant specimens regarding the absence of OP-145 and higher amount of mixed Ag nanospheres (saw TEM image). It was found that PPy/implant in switch (+0.5 V) without incorporating OP-145 showed a much lower antibacterial rate even though a higher amount of Ag nanospheres was mixed, implying that antibacterial rate of this implant system was primarily dependent on the state of OP-145. That was, the antibacterial rate of PPy/implant was insusceptible to the experimentally designed amount of mixed Ag nanospheres.

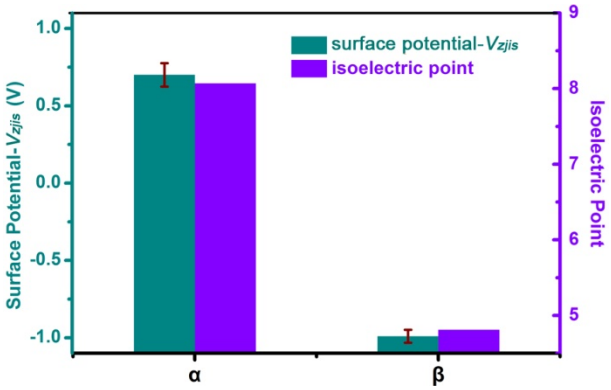


Fig. S21 The plots of surface potential and isoelectric point of PPy/implant. α: after cultivation of MC3T3-E1 osteoblasts for 12 h, PPy/implant in switch (-0.5 V) was rinsed ultrasonically in PBS, ethanol and deionized water for 3 times (each for 10 min) to remove adherent biomolecules and cells, respectively, which was subsequently

applied a potential of +0.50 V. β: after cultivation of *S. aureus* for 12 h, PPy/implant in switch (+0.5 V) was rinsed ultrasonically in PBS, ethanol and deionized water for 3 times (each for 10 min) to remove adherent biomolecules and bacteria, respectively, which was subsequently applied a potential of -0.50 V. It was ascertained that, after cultivation of bacteria (or osteoblasts), the surface chemistry (surface potentials and isoelectric points) of PPy/implant in one state could still be switched to its another state, and therefore was eligible for allowing its next action of promoting osteogenic activity or antibacterial activity.

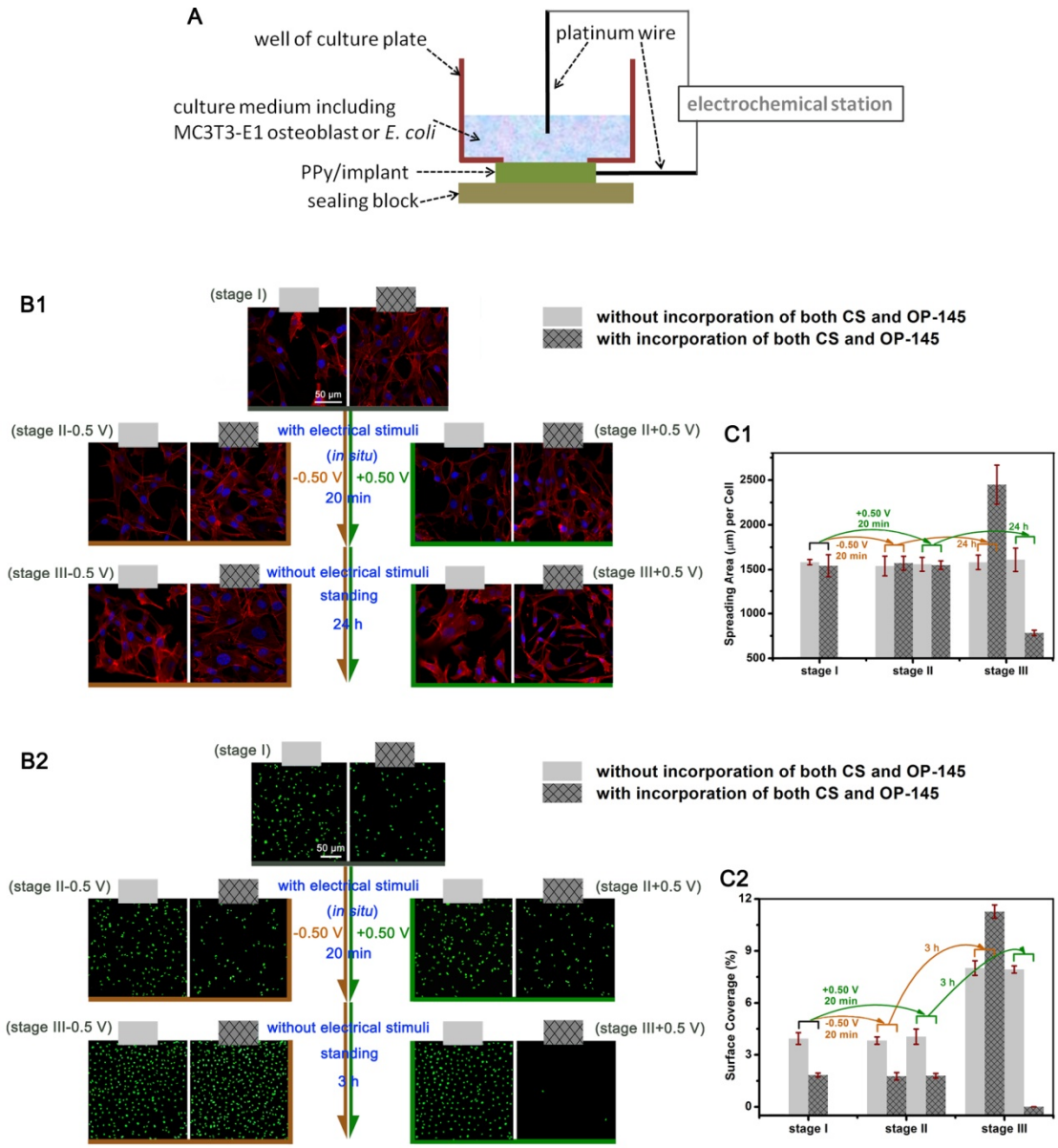


Fig. S22 (A) Schematic illustration of self-designed culture plates for cell culture on PPy/implant where *in situ* electrical stimuli were allowed to applied. A hole was drilled into each well bottom of culture plates, and the

PPy/implant was placed on the bottom from the outside to tightly cover the hole with the assistance of sealing block. The electrochemical station was used to apply electrical stimuli *in situ* to the PPy/implant through two platinum wires, one platinum wire was connected with the PPy/implant, and another one was immersed in the culture medium including MC3T3-E1 osteoblasts or *E. coli*. (B) Fluorescence images of (1) rhodamine labeled phalloidin-stained cytoskeletal actin in MC3T3-E1 osteoblasts (red = F-actin, blue = cell nuclei) and (2) SYTO9 stained *E. coli* adhering on PPy/implant. (C) The plot of (1) spreading area per MC3T3-E1 osteoblast recorded from B1 and (2) surface coverage of adherent *E. coli* analyzed from B2. Before the beginning of all the aforementioned biological tests (as shown in Fig. 3 and 4) of the PPy/implant, the switch states of the PPy/implant were formed in a nonbiological system in advanced. That was, the formation of switch states and their biological tests were respectively conducted in two different and independent systems. To make the biological tests better simulate the *in vivo* use of the PPy/implant in response to electrical stimuli *in situ*, herein the switch states of PPy/implant were expected to form under the presences of MC3T3-E1 osteoblasts or bacteria by applying electrical stimuli *in situ*, and two subsequent stages of early biological behaviours of PPy/implant were discussed in terms of the spreading of osteoblasts and adhesion of bacteria. In this way, the formation of switch states and their biological tests occurred in a biological system. The PPy/implant without incorporation of both CS and OP-145 served as control. Given this, in a self-designed culture plate (Fig. S22A), MC3T3-E1 osteoblasts (seeding density: $5 \times 10^3$) was cultured on the PPy/implant for 18 h (or *E. coli* for 2 h, seeding density: $10^6$ CFU/mL) (staged I in Fig S22B and S22C), and a 20 min of *in situ* electrical stimuli (+0.50 or -0.50 V) was applied to the PPy/implant in culture medium. Just at the completion of response to the 20 min of electrical stimuli (stage II), both the spreading area of osteoblasts and the amount of adherent *E. coli* on the PPy/implant seemed almost the same as stage I. After a standing culture (*i.e.*, without application of electrical stimuli) of osteoblasts for 24 h or *E. coli* for 3 h (stage III), compared with stage I and stage II, the spreading area of osteoblasts on the PPy/implant with incorporation of both CS and OP-145 was found larger in stage III -0.5V (the voltage in stage III -0.5V or stage III +0.5V referred to the electrical stimulus used during the formation of stage II) and smaller in stage III +0.5V, while the amount of adherent *E. coli* became larger in stage III -0.5V and smaller in stage III +0.5V. However, on the PPy/implant without incorporation of both CS and OP-145, both the spreading area of osteoblasts and the amount of adherent *E. coli* showed no different between stage III -0.5V and stage III +0.5V, which possibly resulted from

noneffective switch behaviours of PPy/implant without incorporation of both CS and OP-145 in response to electrical stimuli. This implied that the seeming electrical stimulus-responsive changes in early biological behaviours of osteoblasts and *E. coli* were actually related with electrical stimulus-responsive switch states of the PPy/implant rather than electrical stimuli themselves. Thus, we confirmed that the switch states of the PPy/implant (or the preferential presence of either CS or OP-145 on its surfaces) could be achieved under biological environment by applying electrical stimuli *in situ* and acted directly on the biological behaviours of osteoblasts and *E. coli*.